STIMULATING NEURAL ELECTRODE - A STUDY ON CHARGE INJECTION PROPERTIES OF IRIDIUM OXIDE FILMS

In-Seop Lee
KOREC, #47-3 KooSan-Dong, Pupyong-Ku, Inchon, Korea 403-120
Ray A. Buchanan
Dept. of MS&E, University of Tennessee, Knoxville, TN 37996-2200(USA)
Jim M. Williams
Solid State Division, Oak Ridge National Laboratory, Oak Ridge, TN 37831-6134(USA)

ABSTRACT

For a stimulating neural electrode, the charge density should be as large as possible to provide adequate stimulation of the nervous system while allowing for miniaturization of the electrode. Since iridium oxide is able to produce high charge densities while preventing undesirable reactions due to charge storage, it has become a promising material for neural prostheses. Successful production of stable Ir and Ir oxide films on various substrates now limits the use of this material.

Ir was deposited on two differently prepared surface of (mirror finish, passivation) surgical Ti-6Al-4V with several methods. Ion beam mixing of sputter deposited Ir films on passivated Ti-6Al-4V produced stable and good adherent Ir films. It was found that the increase in charge density of pure Ir on continuous cyclingis due to the accumulation of the oxide phase (associatd with a large surface area) in which the valence state of iridium changes and the double-layer capacitance increases.
This study also showed that the double layer capacitance is equally or even more responsible for the high charge density of anodically formed Ir oxide.

INTRODUCTION

Considerable research has been performed on the electrochemistry of Ir because of its two distinct properties. The first property is associated with its high affinity for hydroxide ions which gives superior catalytic activity for oxygen evolution (1,2). The second property is related to its electrochromic behavior, where a change of color takes place between oxidative and reductive state of the metal, which makes it of interest for use in electro-optic display devices (3-13).

Recently, there is also great interest in Ir for prosthetic applications, especially as an electrical neural stimulation electrode (14-16). Neural prostheses are devices which use electrodes to interface directly with the nervous systems for supplementing or replacing function in the neurologically handicapped (17). The electrical neural stimulation electrode requires a reversible charge injection without causing any neural damage by the formation of toxic faradaic reaction products. It has been found that Ir subjected to repetitive potential sweeps in acid over a certain potential range results in the formation of a thick oxide film and produces as much as a 100-fold increase in the charge injection than a bare Ir electrode (3).

The large charge density of the accumulated iridium oxide, so called "activated Ir" is due to the change in the valence state of iridium atoms (related to electrochromic behavior) on continuous potential cycling (5,18,19). Two different mechanisms have been proposed to explain the electrochromism of the anodic iridium oxide film: the double proton-electron injection mechanism by Gottesfeld et al. (4), and the anion mechanism by Beni et al. (5). Gottesfeld et al. (4) postulated the following reaction to describe the film conversion processes:

$$Ir(OH)_n \leftrightarrow Ir_x(OH)_{n-x} + xH^+ + xe^-$$

In this mechanism, during the coloration process, electrons are removed from the oxide across the metal-oxide interface by application of a suitable anodic potential to the

metal substrate. Charge repulsion causes an equivalent amount of mobile positive charge carriers (protons) to be ejected across the oxide-electrolyte interface, thus preserving electroneutrality inside the oxide. Similary, during bleaching, electrons are injected into the oxide film from the metal while the compensating positive charge is injected at the oxide-electrolyte interface. On the other hand, Beni et al. (5) have observed that the speed of coloration and bleaching in anodic iridium oxide films is independent of pH and the coloration-bleaching process occurs in water-free solutions containing F^- or CN^-. Thus, they have proposed the hydroxide mechanism for anodic iridium oxide film electrochromism, represented by a half reaction of the form:

$$Ir(OH)_3 + x(OH)^- \text{ -- } Ir(OH)_{n+x} + xe^-$$

However, both mechanisms agreed that the coloration is associated with a change in valence of iridium from 3 to 4, and that the reduction of iridium from 4 to 3 relates to the bleaching process.

Robblee et al. (16) studied the charge injection capabilities of thermally-prepared multilayer oxide films on Ti and stated that the large charge density on Ir is the result of faradaic reactions due to the highly reversible H^+ or OH^- transfer reactions and valence transitions within the oxide layer. Also, Foods et al. (20) catalogued IrO_2 as a faradaic stimulation electrode referring to its fast reversible redox reaction. In the present investigation, the increase in charge injection capability of activated Ir was discussed in terms of the capacitance via the faradaic reactions. And Ion beam mixing technique was employed to enhance the interfacial strength of sputter coated iridium films onto Ti-6Al-4V.

EXPERIMENTAL PROCEDURES

Samples of 3/4" in diameter of Ir with thickness of 0.5 mm were cut from plate and the surface were polished through 1 micron diamond paste. Since the samples were subjected to surface analysis by RBS and SEM after electrochemical treatment, the samples were mounted in a specially-constructed Teflon™ sample holder as shown in Figure 1. The resulting sample mount allowed the treated surface to be preserved without any possible mechanical damage. Special care was given to mount the sample such that the electrolyte was not in contact with the sample except at the exposure area of 1 cm^2. The sample-holder/sample-contact areas which could provide a crevice geometry were reduced by sharpening the edges as shown in Figure 1. Teflon™ tape was wrapped around the male

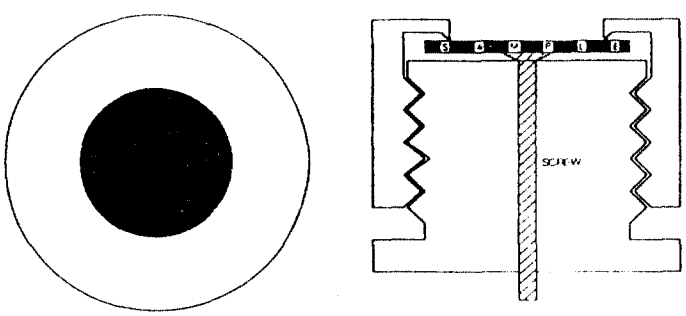

Figure 1. Schematic diagram of the sample holder

part of sample holder to prevent any electrolyte from penetrating into the sample holder. No electrolyte was found inside the sample holder even after several months exposure. The sample was cycled between two potentials at a rate of 100 mV/s and the resultant current density was plotted on a linear scale. The area inside the loop generated by each cycle was measured with a planimeter, and is directly proportional to the charge density (charge per unit area) of the electrode. All cycle voltammetry was performed with an EG&G Princeton Applied Research Model 273 potentiostat.

Ion beam mixing was done onto Ir sputter coated Ti-6Al-4V by use of titanium beam

ions produced by a Varian/Extrion implanter and parameters are shown in Table 1.

Table 1. Ion beam mixing parameters and results

Ir THICKNESS (nm) FROM RBS	NUMBER OF Ir (AS-SPUTTERED)	ENERGY OF Ti MIXING IONS (KeV)	DOSE OF Ti	NUMBER OF Ir (AFTER IBM)
6.6	4.6 X $10^{16}/cm^2$	50	$10^{16}/cm^2$	3.2 X $10^{16}/cm^2$
11.8	8.3 X $10^{16}/cm^2$	100	$10^{16}/cm^2$	6.2 X $10^{16}/cm^2$
18.8	13 X $10^{16}/cm^2$	150	$10^{16}/cm^2$	11 X $10^{16}/cm^2$

RESULTS AND DISCUSSION

Figure 2 shows cyclic voltammograms of Ir in 0.1 M H_2SO_4. The 1 μm surface finished Ir electrode was potentiodynamically cycled between 0.0 V (SHE) and 1.45 V (SHE) with a linear potential sweep rate of 100 mV/s.

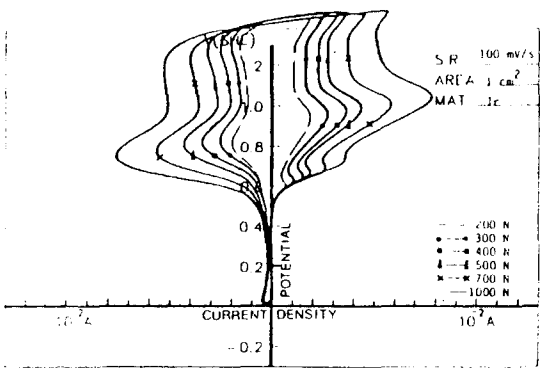

Figure 2. Cyclic voltammograms of an Ir electrode in 0.1M H_2SO_4 (100mV/s)

A very considerable enhancement of the charge densities produced by Ir with increasing number of cycles is shown, and the voltammogram became almost symmetrical with regard to the charge density (i.e. area) about the potential axis. During the anodic sweep, the color of the oxide started changing from metallic to blue around 0.4 V (SHE), became darker and remained dark blue above near 0.9 V (SHE). The bleaching process occurred during the cathodic sweep. The dark blue became lightened around 1.0 V (SHE) and no blue color could be observed below 0.4 V (SHE).

After Ir was activated to a selected number of cycles between 0.0 V (SHE) and 1.45 V (SHE) with a scan rate of 100 mV/s in 0.1 M H_2SO_4, cyclic voltammograms of the activated Ir were determined in the same solution at the same scan rate but between 1.0 V (SHE) and 1.3 V (SHE), over which the change in valence state of Ir does not occur. As shown in Figure 3, the charge density increased with increasing number of cycles.

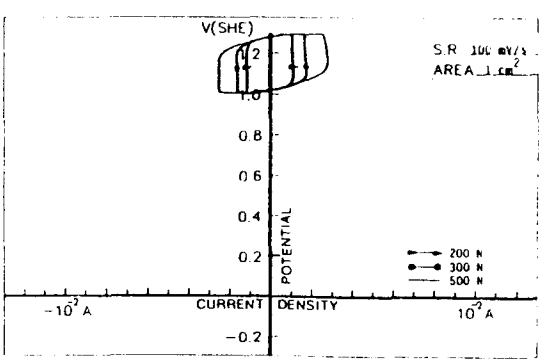

Figure 3. Cyclic voltammograms of Ir between 1.0 V (SHE) and 1.3 V (SHE)

Since there is no valence transition of Ir in this region of potentials, the charge density produced by the activated Ir can not be related to the faradaic reaction. In fact, the activated Ir behaved like a capacitor in these potential range.

Electrochemical impedance spectroscopy (EIS) measurements were performed on pure Ir electrodes, which had been activated to 1 cycle and 200 cycles, at an applied DC potential of 1.2 V (SHE) in 0.1 M H_2SO_4. The Bode plots are shown in Figure 4.

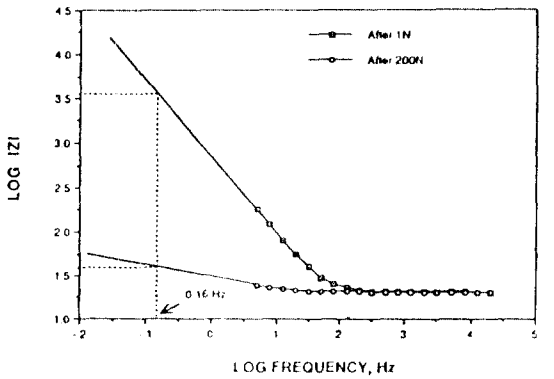

Figure 4. Bode plots for Ir at 1.2 V (SHE) in 0.1 M H_2SO_4

The double layer capacitance was increased from 280 uF to 25 mF for the Ir electrode on going from 1 to 200 cycles. From the relationship shown below for a parallel-plate capacitor,

$$C = Q/V_c = \varepsilon_r \varepsilon_o A/d \text{ farads}$$

where A: the area of the dielectric, m^2
d: the thickness of the dielectric, m
ε_r: the relatiive permittivity of the dieelectric
ε_o: constant, $1/(36\pi \times 10^9)$ farads/m

the area of the dielectric, i.e. the surface area of the anodic oxide film must be increased to account for the higher double layer capacitance assuming a constant thickness of oxide (although the average oxide thickness probably increases, this effect allow would produce lower capacitance values).

Scanning electron mocrographs of Ir activated to the different number of cycles in 0.1 M H_2SO_4 are shown in Figure 5.

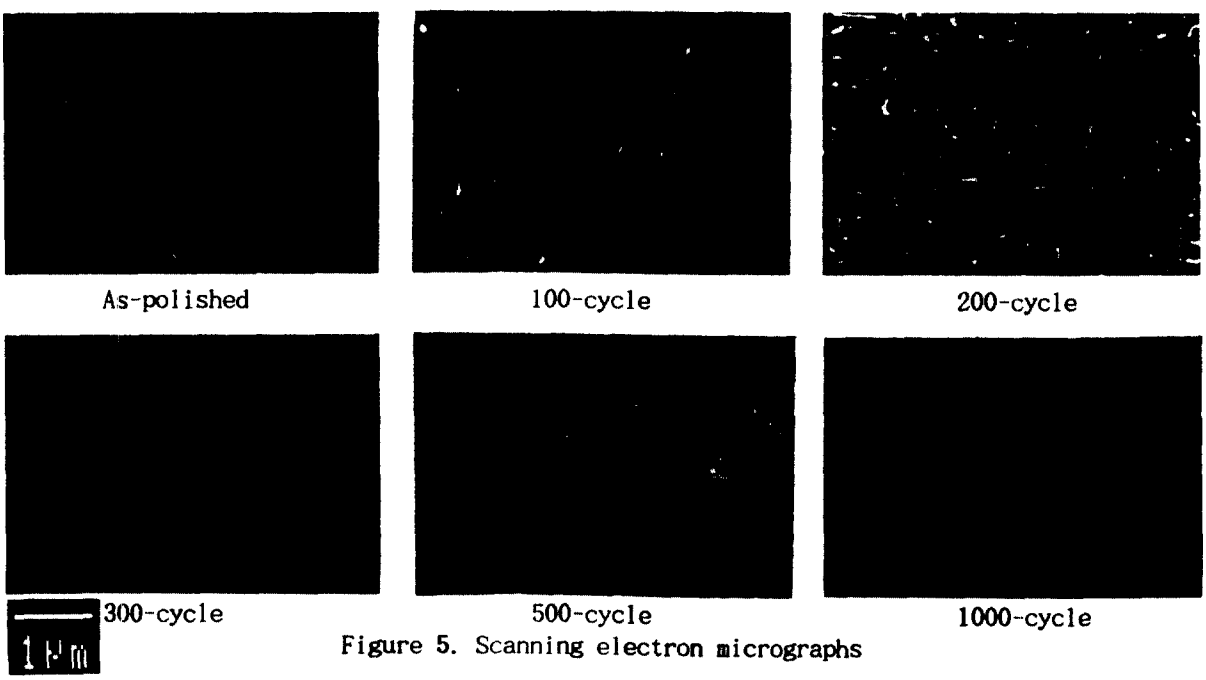

Figure 5. Scanning electron micrographs

It is clearly seen that the oxides were more accumulated on the Ir electrode activatd to higher numbers of cycles. The surface topography of the oxide on Ir cycled to 100-cycle began to show some dissimilarities from the as-polished Ir electrode. With the increase in activating cycles, the surface became more uneven and oxide films of very high real surface area were developed. This roughening was probably due to the strain introduced in the surface layer by virtue of the greater volume occupied by the oxide layer relative to the metal it replaced. Continuous potential cycling for a long period of time may result to the flaking of the oxide. As a matter of fact, the anodic dissolution rate of Ir on potential cycling in 1M H_2SO_4 was claimed to be 8-9 times that found for Pt under comparable experimental conditions (19).

The porous-natured oxide is shown in Figure 6. The oxide morphology possibly allowed the bare Ir to contact with the electrolyte and the oxide to grow continuously with increasing cycles. This oxide was grown on Ir by activating the Ir electrode to 2500 cycles. Whether the underlying regions (marked A in Figure 6) correspond to bare Ir or an oxide layer is not known. However, Rand et al. (19) suggested that a large portion of bare Ir must be exposed since the quantity of charge passed in adsorbing hydrogen, which is a measure of the area of the bare metal surface exposed to the solution (21), decreased by only 25% after Ir was activated to 2500 cycles between 0.06 V (SHE) and 1.5 V (SHE) with sweep rates of 40 mV/s in 1 M H_2SO_4.

Figure 6. Scanning electron micrograph of Ir at 2500-cycle

As shown in Figure 2, the charge density of the activated Ir was mostly produced in the upper portion of each potential cycle even though the morphology of the oxide (high surface area) was not significantly changed with the applied potential at each cycle. EIS measurements were made on Ir activated to 200 cycles, at the applied DC potentials of 0.3 V (SHE) and 1.2 V (SHE). Figure 7 shows the much lower double layer capacitance of Ir at the lower potential. The only possible explanation is the different dielectric properties of the oxides. The higher valence Ir oxide must be characterized by a much higher dielectric constant.

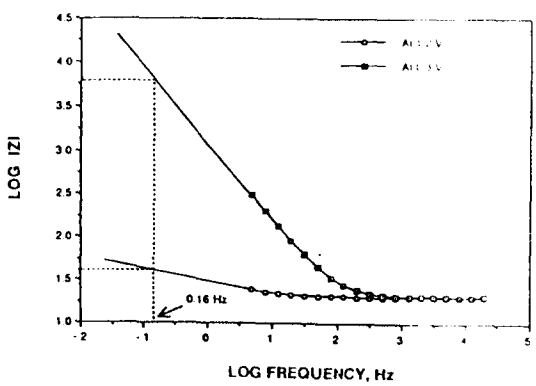

Figure 7. Bode plots of Ir at 0.3 V (SHE) and 1.2 V (SHE)

Figure 8 (a) and (b) show the charge density versus the number of cycles measured from cyclic voltammograms for as-polished samples and for prepassivated samples, respectively.

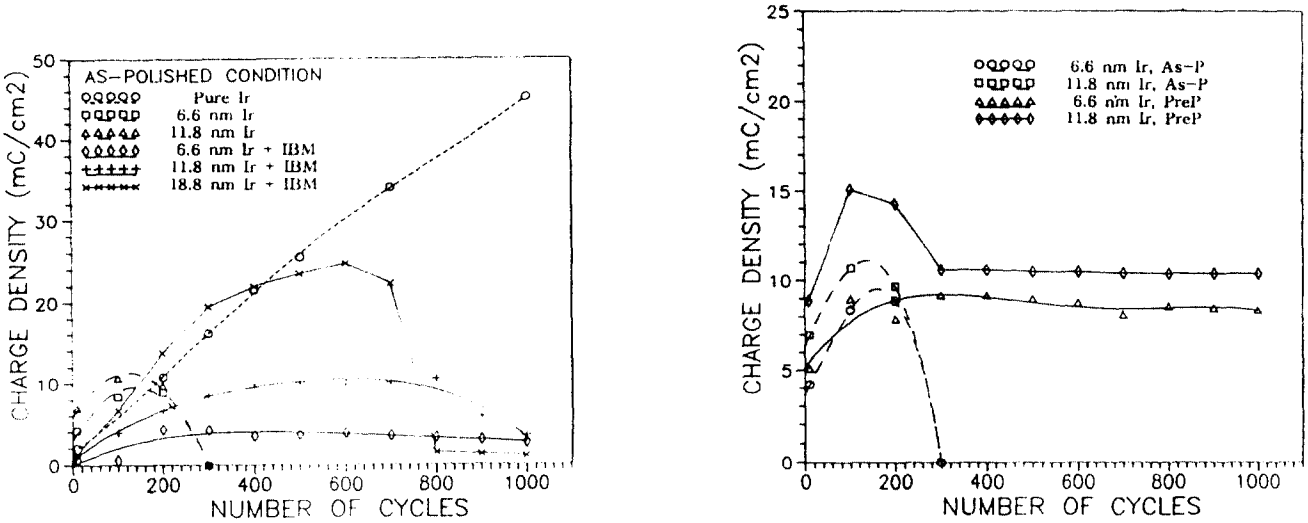

(a) (b)

Figure 8. Charge density versus the number of cycles

For the polished samples, ion beam mixing produced considerable enhancement in the number of cycles in the effective lifetime. Nevertheless, appreciable loss of iridium occurred by about 800 cycles, even for the ion beam mixed samples. The three main factors affecting performance of films for corrosion processes(in contrast to wear) are porosity, adhesion, and stress. For the present films, stress might be a factor because the volume change during activation (addition of oxygen) might make the film tend to be in compression relative to the substrate, and thus to blow up and/or crack. Ion mixing might improve performance in this regard by diffusing the stress field at the interface over a broader range of depths and also by improving adhesion. This effect might explain the better performance of the ion-beam mixed, as-polished samples. Ion mixing might also produce an improvement if porosity of the initially deposited iridium film were a factor. The good adhesion and alloying effects produced by ion mixing could help reduce corrosive undercutting and the resulting spalling initiated at pores and cracks.

The most surprising rsult of the present experiments, however, was that the passivation treatment was as effective as it was in improving the stability of the films. As shown in Figure 8(b), stability was quite good out to 1000 cycles or the duration of the test for the passivated samples. This is especially true in view of the fact that the passivation treatment had little apparent effect in thickening the oxide. RBS analyses showed that the amount of oxygen on the passivated sample does not exceed that on the sample which had been polished only. Because of the small scattering cross-section, the oxygen peak is quite small, but it can nevertheless be estimated that the surface density of oxygen for the mecganically polished sample did not exceed about $2x10^{16}/cm^2$. Mass resolution for the helium-ion RBS technique in this mass range is excellent, however. A limited interpretation is possible because the energy position of these peaks is accurately known, and the scattering yield, though small, can be quantitatively predicted with good accuracy for given proposed surface concentrations of oxygen. Each sample was analyzed, and in no case was oxygen more apparent on a passivated sample than on a mechanically polished sample. Thus, whatever the passivation treatment did, it apparently did not thicken the oxide appreciably. It might be suspected that the strong acid passivation treatment could remove the carbon or other contaminants. Another possible effect could be a change in character of the oxide. Air-formed oxides do not contain hydrogen, but the passivation could produce an oxide

containing OH^-. Such an oxide might be more wettable by deposited iridium than air-formed oxide. Another effect might be less porosity in comparison with the mechanically polished samples. Further analyses are needed to answer many of these questions. Meanwhile we judge that the present data are most compatible with the above tentative hypotheses.

REFERENCES

1. D. N. Buckley and L. D. Burke, J. Chem. Soc. Faraday Trans. 1, 72, 2431 (1976).
2. G. Beni, L. M. Schiavone, J. L. Shay, W. C. Dautremont-Smith, and B. S. Schneider, Nature, 282, 281 (1979).
3. J. O. Zerbino, N. R. De Tacconic, and A. J. Arvia, J. Electrochem. Soc., 125, 1266 (1978).
4. S. Gottesfeld and J. D. E. McIntyre, J. Electrochem. Soc., 126, 742 (1979).
5. G. Beni, C. E. Rice, and J. L. Shay, J. Electrochem. Soc., 127, 1342 (1980)
6. D. Michelle, D. A. J. Rand, and R. Woods, J. Electroanal. Chem., 84, 117 (1977)
7. S. Gottesfeld and S. Srinivasan, J. Electroanal. Chem., 86, 89 (1978)
8. S. Gottesfeld, J. D. E. McIntyre, G. Beni, and J. L. Shay, Appl. Phys. Lett., 33, 208 (1978)
9. L. M. Schiavone, W. C. Dautremonth_Smith, G. Beni, and J. L. Shay, Appl. Phys. Lett., 35, 823 (1979)
10. G. Beni and J. L. Shay, Physical Review B 21, 364 (1980)
11. J. L. Shay, G. Beni, and L. M. Schiavone, Appl. Phys. Lett., 33, 942 (1978)
12. G. Beni and J. L. Shay, Appl. Phys. Lett., 33, 567 (1978)
13. W. C. Dautremont-Smith, G. Beni, L. M. Schiavone, and J. L. Shay, Appl. Phys. Lett., 35, 565 (1979)
14. L. S. Robblee, J. L. Lefko, and S. B. Brummer, J. Electrochem. Soc., 130, 731 (1983)
15. L. S. Robblee, J. Marston, J. Mchardy, and S. B. Brummer, Biomaterials, 1, 135 (1980)
16. L. S. Robblee; M. J. Mangaudis, E. D. Lasinsky, A. G. Kimball, and S. B. Brummer, in Biomedical Materials, J. M. Williams, M. F. Nichols, and W. Zingg eds., MRS 55, 303 (1986)
17. F. T. Hambrecht, in Biomedical Materials, J. M. Williams, M. F. Nichols, and W. Zingg eds., MRS 55, 265 (1986)
18. M. Vukovic, J. Appl. Electrochem., 17, 737 (1987)
19. D. A. J. Rand and R. Woods, J. Electroanal. Chem., 55, 375 (1974)
20. J. S. Foods and S. M. Erker, in Biomedical Materials, J. M. Williams, M. F. Nichols, and W. Zingg eds., MRS 55, 281 (1986)
21. R. Woods, J. Electroanal. Chem., 49, 217 (1974)
22. S. B. Brummer, L. S. Robblee, and F. T. Hambrecht, Annals of the New York Academy of Science, 405, New York Academy of Science, New York, 159 (1983)